


Novel Majeed Syndrome–Causing *LPIN2* Mutations Link Bone Inflammation to Inflammatory M2 Macrophages and Accelerated Osteoclastogenesis

Farzana Bhuyan,¹ Adriana A. de Jesus,¹ Jacob Mitchell,¹ Evgenia Leikina,² Rachel VanTries,¹ Ronit Herzog,³ Karen B. Onel,⁴ Andrew Oler,¹ Gina A. Montealegre Sanchez,¹ Kim A. Johnson,¹ Lena Bichell,¹ Bernadette Marrero,¹ Luis Fernandez De Castro,⁵ Yan Huang,¹ Katherine R. Calvo,⁶ Michael T. Collins,⁵ Sundar Ganesan,¹ Leonid V. Chernomordik,² Polly J. Ferguson,⁷ and Raphaela Goldbach-Mansky¹ 

Objective. To identify novel heterozygous *LPIN2* mutations in a patient with Majeed syndrome and characterize the pathomechanisms that lead to the development of sterile osteomyelitis.

Methods. Targeted genetic analysis and functional studies assessing monocyte responses, macrophage differentiation, and osteoclastogenesis were conducted to compare the pathogenesis of Majeed syndrome to interleukin-1 (IL-1)–mediated diseases including neonatal-onset multisystem inflammatory disease (NOMID) and deficiency of the IL-1 receptor antagonist (DIRA).

Results. A 4-year-old girl of mixed ethnic background presented with sterile osteomyelitis and elevated acute-phase reactants. She had a 17.8-kb deletion on the maternal *LPIN2* allele and a splice site mutation, p.R517H, that variably spliced out exons 10 and 11 on the paternal *LPIN2* allele. The patient achieved long-lasting remission receiving IL-1 blockade with canakinumab. Compared to controls, monocytes and monocyte-derived M1-like macrophages from the patient with Majeed syndrome and those with NOMID or DIRA had elevated caspase 1 activity and IL-1 β secretion. In contrast, lipopolysaccharide-stimulated, monocyte-derived, M2-like macrophages from the patient with Majeed syndrome released higher levels of osteoclastogenic mediators (IL-8, IL-6, tumor necrosis factor, CCL2, macrophage inflammatory protein 1 α/β , CXCL8, and CXCL1) compared to NOMID patients and healthy controls. Accelerated osteoclastogenesis in the patient with Majeed syndrome was associated with higher NFATc1 levels, enhanced JNK/MAPK, and reduced Src kinase activation, and partially responded to JNK inhibition and IL-1 (but not IL-6) blockade.

Conclusion. We report 2 novel compound heterozygous disease-causing mutations in *LPIN2* in an American patient with Majeed syndrome. *LPIN2* deficiency drives differentiation of proinflammatory M2-like macrophages and enhances intrinsic osteoclastogenesis. This provides a model for the pathogenesis of sterile osteomyelitis which differentiates Majeed syndrome from other IL-1–mediated autoinflammatory diseases.

INTRODUCTION

Genetically defined autoinflammatory bone diseases are caused by dysregulation of innate immune responses resulting

in systemic inflammation (1) and osteomyelitis, which includes Majeed syndrome, caused by recessive loss-of-function mutations in *LPIN2* (2), and deficiency of interleukin-1 (IL-1) receptor antagonist (DIRA), caused by loss-of-function mutations in *IL1RN*

ClinicalTrials.gov identifier: NCT02974595.

Supported by the Intramural Research Programs of the National Institute of Allergy and Infectious Diseases and the Eunice Kennedy Shriver National Institute of Child Health and Human Development, NIH. Dr. Ferguson's work was supported by the National Institute of Arthritis and Musculoskeletal and Skin Diseases, NIH (grant R01-AR-059703).

¹Farzana Bhuyan, PhD, Adriana A. de Jesus, MD, PhD, Jacob Mitchell, BS, Rachel VanTries, BS, Andrew Oler, PhD, Gina A. Montealegre Sanchez, MD, Kim A. Johnson, BS, Lena Bichell, BS, Bernadette Marrero, PhD, Yan Huang, MD, Sundar Ganesan, PhD, Raphaela Goldbach-Mansky, MD, MHS: National Institute of Allergy and Infectious Diseases, NIH, Bethesda, Maryland; ²Evgenia Leikina, DVM, Leonid V. Chernomordik, PhD: Eunice Kennedy Shriver National Institute of Child Health and Human Development, NIH, Bethesda, Maryland; ³Ronit Herzog, MD: NYU Langone Medical Center, New

York, New York; ⁴Karen B. Onel, MD: Hospital for Special Surgery, New York, New York; ⁵Luis Fernandez De Castro, PhD, Michael T. Collins, MD: National Institute of Dental and Craniofacial Research, NIH, Bethesda, Maryland; ⁶Katherine R. Calvo, MD, PhD: NIH Clinical Center, NIH, Bethesda, Maryland; ⁷Polly J. Ferguson, MD: University of Iowa Carver College of Medicine, Iowa City.

Drs. Bhuyan and de Jesus contributed equally to this work.

Dr. Goldbach-Mansky has received research grants from Eli Lilly and Sobi. No other disclosures relevant to this article were reported.

Address correspondence to Raphaela Goldbach-Mansky, MD, MHS, or Farzana Bhuyan, PhD, NIH, 10 Center Drive, Bethesda, MD 20892. Email: farzana.bhuyan@nih.gov or goldbacr@mail.nih.gov.

Submitted for publication May 1, 2020; accepted in revised form December 10, 2020.

encoding the IL-1 receptor (IL-1R) antagonist (3,4). Majeed syndrome presents in early childhood with osteitis and osteomyelitis, dyserythropoietic anemia, and elevation of acute-phase reactants. Since its initial description in 1989 (5), 23 patients from 10 families/kindreds of Jordanian, Indian, Arabic, Turkish, and Chinese ethnic backgrounds have been described as having 7 autosomal-recessive, disease-causing loss-of-function mutations (summarized in Supplementary Table 1, available on the *Arthritis & Rheumatology* website at <http://onlinelibrary.wiley.com/doi/10.1002/art.41624/abstract>). Clinical similarities to DIRA and a rapid resolution of the inflammatory disease manifestations upon treatment with short- and long-acting IL-1 inhibitors suggest a prominent role of IL-1 in disease pathogenesis (6,7).

LPIN2 encodes lipin 2, a magnesium-dependent phosphatidic acid phosphatase enzyme that associates with membrane lipids and localizes to organelles. Lipin 2 catalyzes the conversion of phosphatidic acid to diacylglycerol (DAG) and acts as a branch point for the synthesis of triacylglycerol and phospholipids (8–12). Recently, a link between lipin 2 deficiency and inflammation was described (13). Lipin 2 negatively regulates MAPK phosphorylation and contributes to the activation of the NLRP3 inflammasome. Bone marrow-derived macrophages (BMMs) from *Lpin2*^{-/-} mice or small interfering RNA-induced silencing of *Lpin2* in murine and human macrophages showed increased IL-1 production in response to stimulation with lipopolysaccharide (LPS) and ATP (13). Reduced lipin 2 levels, as seen in patients with Majeed syndrome with disease-causing loss-of-function mutations, result in a decrease in cellular cholesterol levels, which increases ion currents through the ATP-activated P2X₇ receptor and subsequent NLRP3 inflammasome activation with mature IL-1 β release (13).

Despite insights that link *LPIN2* mutations to increased pro-IL-1 β transcription and to NLRP3 inflammasome activation, pathomechanisms that provide insight into the differential development of osteomyelitis in Majeed syndrome and DIRA (but not in the NLRP3 inflammasomopathy, neonatal-onset multisystem inflammatory disease [NOMID]) remain unresolved (Supplementary Figure 1, <http://onlinelibrary.wiley.com/doi/10.1002/art.41624/abstract>) and suggest NLRP3 inflammasome-independent effects of *LPIN2* in regulating bone homeostasis at the growth plate of long bones. In the present study we demonstrated that *LPIN2* mutations differentially affect monocytes, monocyte-derived M1-like macrophages (M1-MDMs) and M2-MDMs, and osteoclastogenesis in the various IL-1-mediated diseases. In contrast to the NLRP3 inflammasomopathy, NOMID, LPS-stimulated M2-MDMs from patients with Majeed syndrome and DIRA are inflammatory, and the mutations promote accelerated osteoclastogenesis. These effects were mediated through changes in phosphorylation patterns in macrophages in the patient with Majeed syndrome and could largely be reversed through IL-1 inhibition. Our data suggest a novel role of lipin 2 in macrophage

polarization and osteoclastogenesis, and we propose a disease model for sterile osteomyelitis.

PATIENTS AND METHODS

Patients. The parents of the patient with Majeed syndrome and the adult healthy control donors provided written informed consent. Patients were enrolled in an institutional review board-approved National Institutes of Health (NIH) natural history protocol (Clinical Trials.gov identifier: NCT02974595). Blood samples were collected. Further details about all methods described in this section are presented in Supplementary Methods (<http://onlinelibrary.wiley.com/doi/10.1002/art.41624/abstract>).

Genetic analyses. Targeted sequencing. Clinical genetic testing of *ELANE*, *LPIN2*, *MEFV*, *MVK*, *NLRP3*, *PSTPIP1*, and *TNFRSF1A* (GeneDx) was inconclusive.

Array-based comparative genomic hybridization (aCGH). Genomic DNA from the mother of the patient with Majeed syndrome was examined by aCGH using the current version of ExonArrayDx (GeneDx).

Deletion breakpoint delineation by polymerase chain reaction (PCR) and Sanger sequencing. Serial forward and reverse primers close to the 5' and 3' ends of the deletion, respectively, were designed to obtain new amplicons. PCR products were sequenced in both directions using an ABI 3100 Genetic Analyzer (Applied Biosystems).

Detection of *LPIN2* splicing abnormalities by complementary DNA (cDNA) PCR and sequencing. Complementary DNA primers were designed using Primer3Plus to amplify the region between exon 8 and exon 12 of *LPIN2* NM_014646.2.

***LPIN2* transcript quantification in RNA-Seq data using StringTie.** Raw reads were mapped to the reference human genome (hg19) by TopHat (version 2.0.8; <https://ccb.jhu.edu/software/tophat/index.shtml>), and we assembled transcripts and determined normalized expression values for each spliced event using StringTie (version 1.3.3).

Cell culture experiments. Differentiation of human monocytes and monocyte-derived macrophages. Human peripheral blood-derived monocytes and macrophages were prepared from heparinized venous blood as previously described (14). Peripheral blood mononuclear cells (PBMCs) were suspended in RPMI 1640 medium containing a low concentration (1%) of fetal bovine serum (FBS). Adherent monocytes were seeded in multi-well plates or dishes; they were differentiated into M1-MDMs and M2-MDMs by culturing with RPMI 1640 supplemented with 10% FBS containing either 10 ng/ml recombinant human granulocyte-macrophage colony-stimulating factor (GM-CSF) (for M1-MDMs) or 100 ng/ml recombinant human M-CSF (for M2-MDMs) (both from PeproTech). After 3 days, media were replaced with either

GM-CSF or M-CSF, and fresh complete media and cells were incubated for another 2 or 3 days.

Osteoclast differentiation and pit formation assay. Osteoclasts were prepared from peripheral blood-derived monocytes (15). Briefly, PBMCs from the patient with Majeed syndrome and the controls were suspended in α -minimum essential medium (α -MEM) containing 1% FBS. Monocytes were enriched by allowing attachment to plates and were cultured in α -MEM containing 10% FBS with M-CSF (100 ng/ml) for 6 days; floating cells were removed, and the attached MDMs were used as osteoclast precursors. To generate osteoclasts, M-CSF macrophages were cultured with combinations of M-CSF (100 ng/ml) and RANKL (30 ng/ml). After an additional 3–6 days of culture, cells were fixed and stained for tartrate-resistant alkaline phosphatase (TRAP) (Cosmo Bio). TRAP-positive multinucleated cells containing >3 nuclei were considered TRAP-positive multinuclear osteoclasts.

For the pit assay, harvested cells were inoculated on fluorescein-labeled CaP-coated 24-well plates at a density of 1×10^4 cells/well (Cosmo Bio), and were cultured for an additional 3–6 days with M-CSF (100 ng/ml) and RANKL (30 ng/ml) according to the manufacturer's recommendation. After 6 days, plates were washed with phosphate buffered saline and treated with 5% sodium hypochlorite for 5 minutes. After washing the plates, 5 different regions in each well were photographed by microscopy, and the pit areas were measured with ImageJ software.

Stimulation/inhibition assays. Adherent monocytes, M1-MDMs, or M2-MDMs were stimulated in the presence of LPS (1 μ g/ml) for 2 hours and 30 minutes followed by 30-minute stimulation with ATP (1 mmole) (Sigma-Aldrich). After 24 hours, culture supernatants were collected. For blocking assays, the following were used: IL-1 inhibitor anakinra (Sobi), potent JNK inhibitor SP600125 or phosphorylation of JNK (InvivoGen), macrophage migration inhibitory factor (MIF) inhibitor ISO-1 (R&D Systems), potent tumor necrosis factor (TNF) inhibitor SPD304 (Sigma-Aldrich), and IL-6 inhibitor tocilizumab (Genentech).

Cytokine/chemokine production and enzyme-linked immunosorbent assay (ELISA). Relative levels of multiple cytokines and chemokines in the supernatants of macrophages were analyzed using a proteome profiler human cytokine array according to the instructions of the manufacturer (R&D Systems). Briefly, culture supernatants (200 μ l) of macrophages, which were collected after centrifugation, were added to dot-blots onto which the captured antibodies had been spotted in duplicate. After incubation with the secondary antibody mixture, the resultant signals were detected using a Bio-Rad image analyzer. A total of 36 cytokines, chemokines, and acute-phase proteins can be screened (16,17). The intensity of the spots was quantified using ImageJ software. In order to assess concentrations of IL-1 α , IL-1 β , and IL-10, the supernatants of macrophages stimulated in the presence or absence of LPS and ATP were collected and analyzed by ELISA (R&D Systems).

Phosphokinase array. A human Phospho-Kinase Array Kit (no. ARY003B; R&D Systems) was used to simultaneously detect the relative site-specific phosphorylation of 43 kinases. Briefly, cells were plated and cultured for M2-MDM differentiation with M-CSF (100 ng/ml), and 0.5×10^6 cells were lysed and assayed according to the manufacturer's instructions. The array results were quantified using ImageJ software.

Immunofluorescence staining. Stimulated and unstimulated macrophages were fixed in 4% paraformaldehyde, permeabilized with 0.1% Triton X-100, and stained with a single antibody or combinations of anti-gasdermin D antibody (no. LS-B4537; LifeSpan Biosciences), anti-caspase 1 antibody (no. ab-1872; Abcam), anti-lipin 2 antibody (no. HPA017857; Sigma-Aldrich), anti-RANK antibody (no. ab222215; Abcam), and anti-IL-1R1 antibody (no. ab106278; Abcam) for 12 hours, followed by Alexa Fluor 568-conjugated anti-mouse IgG antibody (Invitrogen) or Alexa Fluor 488-conjugated anti-rabbit IgG antibody (Abcam). DAPI (Molecular Probes) was used to visualize nuclei. Signals were visualized with a confocal laser scanning microscope (Leica SP8). Image processing was performed with Imaris 9.2.1 software.

Statistical analysis. Statistical analyses and graphing were performed using GraphPad Prism 6. Differences in unpaired data with parametric or nonparametric distributions were analyzed by Student's *t*-test and Mann-Whitney U test, respectively, assuming the same variance for each group. *P* values were not corrected for multiple comparisons and must be viewed as exploratory.

RESULTS

Majeed syndrome in 4-year-old patient caused by 2 novel compound heterozygous mutations in *LPIN2*.

A 4-year-old female patient of Puerto Rican and African American descent was evaluated at the NIH for suspected Majeed syndrome (Supplementary Results, <http://onlinelibrary.wiley.com/doi/10.1002/art.41624/abstract>). A radiograph of the right knee obtained at 26 months to evaluate recurrent right knee pain revealed horizontal lucencies at the distal femur and proximal tibia. Laboratory examinations showed systemic inflammation with elevated erythrocyte sedimentation rate (ESR) (55 mm/hour) and C-reactive protein (CRP) level (61 mg/liter), and a knee magnetic resonance imaging demonstrated an abnormal bone marrow signal in the bilateral distal femoral metaphyses (Figure 1B).

The patient had anemia, and a bone marrow biopsy showed 70–90% marrow cellularity with trilineage hematopoiesis and dyserythropoietic, binuclear erythrocyte precursors (Supplementary Figure 2, <http://onlinelibrary.wiley.com/doi/10.1002/art.41624/abstract>). At the first NIH visit at the age of 4 years, the laboratory examination showed mild anemia with the following test results: hemoglobin 10.1 gm/dl (normal 10.2–12.7), mean corpuscular

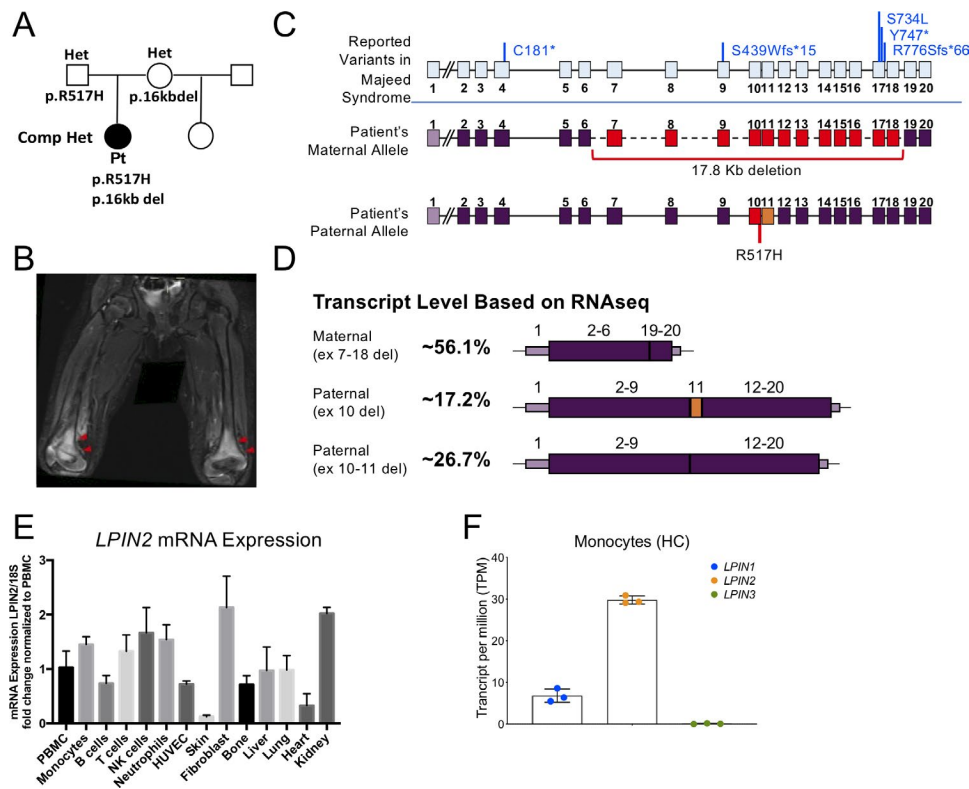


Figure 1. Novel mutations in *LPIN2* cause a compound heterozygous form of Majeed syndrome. **A**, The patient with Majeed syndrome was compound heterozygous (Comp Het) for 2 rare variants in *LPIN2*. **B**, Magnetic resonance imaging (STIR imaging) of the patient's knee shows bone marrow enhancement without cortical lesions. **C**, Genomic structure is shown along with location of the *LPIN2* locus and known disease-causing *LPIN2* variants reported in the literature (blue). The patient's maternal allele is depicted with deleted exons (red), while the paternal allele is depicted with splice site mutations, including spliced out exon 10 (red) or exons 10 and 11 (orange). **D**, *LPIN2* splice junctions were quantified in the patient's blood using alignment data on whole-blood RNA-Seq analysis, yielding predicted transcript levels with each deletion (healthy control [HC] data not shown). Prediction of 56% of the transcript with the maternal deletion suggests that this mutation confers protection against nonsense-mediated mRNA decay; the 2 alternatively spliced transcripts lacked either exon 10 alone (17.2% of the transcript) or exons 10 and 11 (26.7% of the transcript). **E**, *LPIN2* mRNA expression in human cell subsets and tissues was quantified by real-time quantitative polymerase chain reaction. Fold changes in *LPIN2* expression (relative to *18S*) are shown; bars show the mean \pm SD of 3 technical replicates. **F**, Levels of *LPIN1*, *LPIN2*, and *LPIN3* mRNA were quantified by RNA-Seq analysis in human monocytes from healthy controls; bars show the mean \pm SD of 3 samples. PBMC = peripheral blood mononuclear cell; NK = natural killer; HUVEC = human umbilical vein endothelial cell.

volume 65.2 fl (normal 72.3–85), thrombocytosis with platelets 556 K/ μ l (normal 189–394), and systemic inflammation (ESR 77 mm/hour [normal <15] and CRP 104 mg/liter [normal <5]). After intermittent short courses of nonsteroidal antiinflammatory drugs, the patient was started on treatment with the monoclonal anti-IL-1 β antibody, canakinumab, at 2 mg/kg every 8 weeks. She has continued to receive treatment for the past 6.5 years, with significant clinical and laboratory improvement (Supplementary Table 2, <http://onlinelibrary.wiley.com/doi/10.1002/art.41624/abstract>).

The clinical features and treatment response suggested an autoinflammatory bone disease, and genetic testing identified a previously unidentified mutation in *LPIN2*, c.1550G>A, p.R517H, a variant that was initially thought to be homozygous. The presence of the missense variant in the patient's father but not her mother prompted a search for a large deletion that revealed a multiexon deletion spanning exons 7–18, which was

confirmed by aCGH of the maternal DNA (Figure 1C). PCR and Sanger sequencing of the approximate breakpoint regions that were identified by aCGH demonstrated a 17,770-bp deletion (Chr18: 2,921,149–2,938,919) (Supplementary Figures 3A–C, <http://onlinelibrary.wiley.com/doi/10.1002/art.41624/abstract>). Sequencing primers to detect the deletion are listed in Supplementary Figure 3D. RNA-Seq transcripts were quantified, and the presence of 56% of all *LPIN2* transcripts with the maternal deletion suggests protection against nonsense-mediated messenger RNA (mRNA) decay.

To investigate aberrant splicing by the paternally inherited mutation in exon 10, we sequenced *LPIN2* cDNA between exons 8 and 12 and detected 2 alternatively spliced transcripts with deleted exon 10 or deleted exons 10 and 11 in the patient's and her father's cDNA (Supplementary Figure 3E). RNA-Seq expression levels of the alternatively spliced transcripts lacking exon 10 alone were estimated to be ~17%, and ~27%

of transcripts lacked exons 10 and 11 (Figure 1D). *LPIN2* was widely expressed, including in myeloid cells (Figure 1E), and of the 3 lipins, monocytes almost exclusively expressed *LPIN2* (Figure 1F). Using commercial antibodies that are directed to the C-terminal domain (which was deleted in the mutation from the patient's mother), we detected ~50% of normal lipin 2 protein expression in patient cells, which was likely from the paternal splice variants (data not shown).

Lipin 2 mutations cause constitutive inflammasome activation and high IL-1 β production in patient monocytes and M1-MDMs. Previously, serum IL-1 β levels were reported to be elevated in patients with Majeed syndrome who had lipin 2 mutations (6) and in macrophages from *Lpin2*^{-/-} mice (13). We assessed IL-1 β production in LPS- and ATP-stimulated monocytes and in M1-MDMs and M2-MDMs, comparing the patient with Majeed syndrome to disease controls and healthy controls. Increased inflammasome activation and IL-1 β secretion were observed on 2 separate visits in the patient with Majeed syndrome, despite receiving canakinumab. IL-1 β release in monocytes was elevated to a level similar to that observed in patients with the IL-1-mediated autoinflammatory osteomyelitis syndrome (DIRA) but lower than that observed in patients with the IL-1-mediated inflammasomopathy (NOMID), which does not present with osteomyelitis (Figure 2A). IL-1 β release was blocked by the recombinant IL-1 receptor antagonist, anakinra (shown in monocytes) (Figure 2B). In contrast to monocytes, unstimulated M1-MDMs and M2-MDMs from the patient with Majeed syndrome and patients with DIRA exhibited elevated IL-1 β levels, and LPS- and ATP-stimulated IL-1 β secretion was also increased in M1-MDMs, but not in M2-MDMs, in the patient with Majeed syndrome (Figure 2C).

Consistent with these observations, caspase 1 and gasdermin D expression were up-regulated in M1-MDMs in the patient with Majeed syndrome, but gasdermin D expression in M2-MDMs was comparable to that in healthy controls (Supplementary Figure 4 and Supplemental Movie 1, <http://onlinelibrary.wiley.com/doi/10.1002/art.41624/abstract>). In contrast, LPS- and ATP-stimulated M1-MDMs and M2-MDMs from NOMID patients secreted significantly more IL-1 β than healthy controls (Figures 2C and D). While LPS- and ATP-stimulated IL-1 α secretion was variable in monocytes and M1-MDMs, IL-1 α tended to be higher in stimulated M2-MDMs from the patient with Majeed syndrome and those with DIRA, but not in NOMID M2-MDMs (Supplementary Figure 5, <http://onlinelibrary.wiley.com/doi/10.1002/art.41624/abstract>).

Proinflammatory M2-MDMs from the patient with Majeed syndrome compared to patients with NOMID and healthy controls. Monocytes from the patient with Majeed syndrome differentiated normally into M1-MDMs and M2-MDMs. While M2-MDMs expressed low levels of CD80 (M1-MDM marker), similar to controls, they had lower expression of

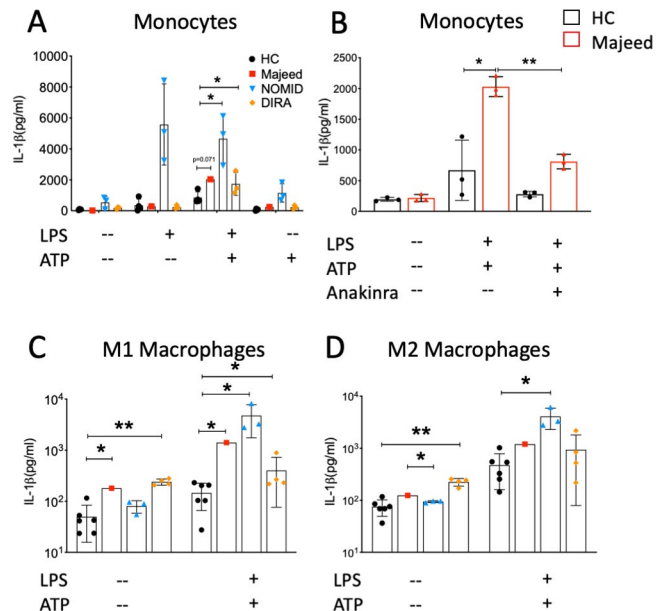


Figure 2. Effect of disease-causing *LPIN2* mutations on interleukin-1 β (IL-1 β) production in monocytes and macrophages. IL-1 β concentration in supernatant was analyzed by enzyme-linked immunosorbent assay. **A**, Adherent monocytes from peripheral blood mononuclear cells were stimulated with lipopolysaccharide (LPS; 1 μ g/ml) for 2.5 hours and ATP (1 mmole) for 30 minutes. Each symbol represents an individual subject: healthy controls (HCs) ($n = 4$), patient with Majeed syndrome ($n = 1$), patients with neonatal-onset multisystem inflammatory disease (NOMID) ($n = 3$), and patients with deficiency of the IL-1 receptor antagonist (DIRA) ($n = 3$). Bars show the mean \pm SD. Values from the patient with Majeed syndrome represent the mean of 3 technical replicates. **B**, LPS- and ATP-stimulated monocytes were cultured in the presence or absence of anakinra (10 mg/ml). Each symbol represents an individual subject: healthy controls ($n = 3$) and patient with Majeed syndrome ($n = 1$). Bars show the mean \pm SD. Values from the patient with Majeed syndrome were obtained from 3 independent experiments, using samples from separate visits, with the mean of 2 technical replicates shown. **C** and **D**, M1-like macrophages (**C**) and M2-like macrophages (**D**) were stimulated with LPS (1 μ g/ml) and ATP (1 mmole) for 24 hours. Each symbol represents an individual subject: healthy controls ($n = 6$), patient with Majeed syndrome ($n = 1$), patients with NOMID ($n = 3$), and patients with DIRA ($n = 4$). Bars show the mean \pm SD. Values for the patient with Majeed syndrome represent the mean of the technical replicates. * = $P < 0.05$; ** = $P < 0.001$, by 2-sample *t*-test assuming equal variances to compare disease groups, or by Student's unpaired *t*-test to compare stimulation with anakinra to no stimulation with anakinra.

CD163 (M2-MDM marker) compared to M2-MDMs from healthy controls (Supplementary Figure 6, <http://onlinelibrary.wiley.com/doi/10.1002/art.41624/abstract>). To assess responses of M1-MDMs and M2-MDMs to inflammatory stimuli, cytokine and chemokine profiles were compared among LPS- and ATP-stimulated M1-MDMs and M2-MDMs from the patient with Majeed syndrome and those with NOMID or DIRA (Figures 3A and B). IL-8 was constitutively expressed in the M2-MDMs but not the M1-MDMs from the patient with Majeed syndrome and from 1 of 4 DIRA patients.

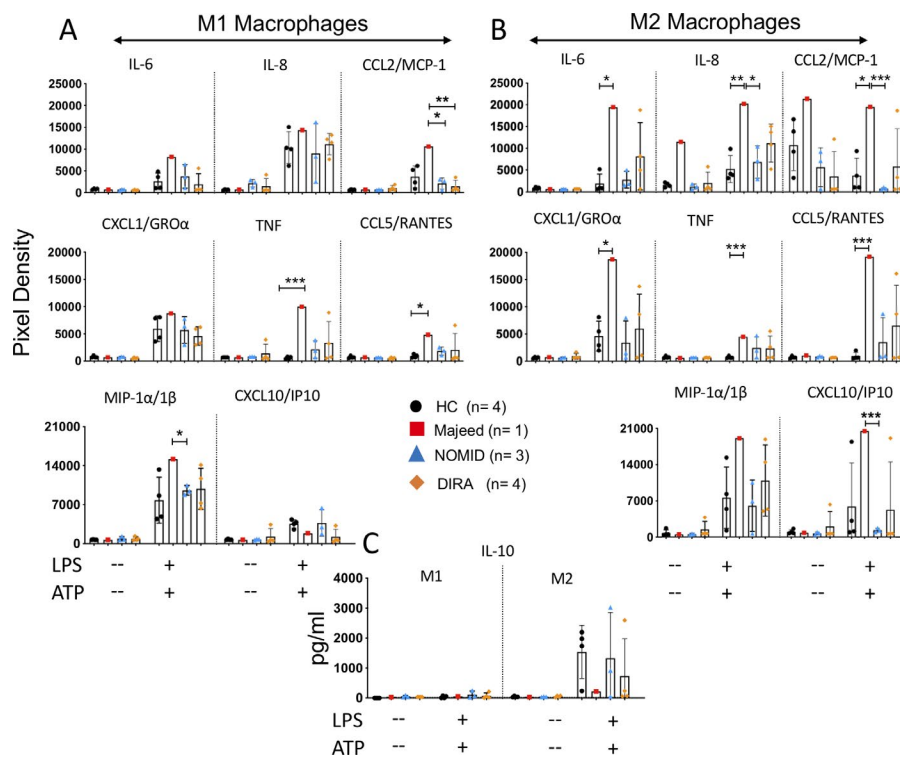


Figure 3. Cytokine and chemokine production upon stimulation of M1-like macrophages (M1-MDMs) and M2-MDMs. **A** and **B**, M1-MDMs (**A**) and M2-MDMs (**B**) were stimulated with LPS (1 μ g/ml) and ATP (1 mmole) for 24 hours. The relative levels of various cytokines and chemokines in supernatant were analyzed by antibody array, and cytokine density was analyzed using ImageJ software. **C**, IL-10 levels were analyzed by enzyme-linked immunosorbent assay. Each symbol represents an individual subject: healthy controls (n = 4), patient with Majeed syndrome (n = 1), patients with NOMID (n = 3), and patients with DIRA (n = 4). Bars show the mean \pm SD. Values from the patient with Majeed syndrome represent the mean of 2 technical replicates. * = $P < 0.05$; ** = $P < 0.001$; *** = $P < 0.0001$, by 2-sample t -test assuming equal variances. MCP-1 = monocyte chemoattractant protein 1; GRO α = growth-related oncogene α ; TNF = tumor necrosis factor; MIP-1 α / β = macrophage inflammatory protein 1 α / β ; IP-10 = interferon- γ -inducible protein 10 (see Figure 2 for other definitions).

Compared to healthy controls and NOMID patients, the M2-MDMs from the patient with Majeed syndrome secreted more IL-6 and IL-8 in response to LPS stimulation, which was most similar to the DIRA patients. TNF elevation was higher in M1-MDMs than in M2-MDMs from the patient with Majeed syndrome compared to healthy controls; however, levels in M2-MDMs from the patient with Majeed syndrome and patients with NOMID or DIRA were similar. Higher secretion of chemokines, including CXCL1/growth-related oncogene α (GRO α), macrophage inflammatory protein 1 α / β (MIP-1 α / β), CCL5/RANTES, and CXCL10, was observed in LPS- and ATP-stimulated M2-MDMs from the patient with Majeed syndrome compared to unstimulated macrophages as well as stimulated disease control macrophages (Figures 3A and B). IL-10 production by M2-MDMs from the patient with Majeed syndrome and 3 of 4 DIRA patients was lower compared to healthy controls and NOMID patients (Figure 3C).

Enhanced osteoclastogenesis in the patient with Majeed syndrome compared to healthy controls and patients with NOMID. Although many of the proinflammatory cytokine/chemokines that are up-regulated in Majeed syndrome promote osteoclastogenesis (18–21), we hypothesized that the

LPIN2 mutations may promote osteoclastogenesis independently of external cytokine supplementation. M2-MDMs are osteoclast precursors (22,23) that differentiate into osteoclasts upon RANKL stimulation. In fact, higher numbers of monocyte-derived TRAP-positive osteoclasts were derived from M2-MDMs from the patient with Majeed syndrome compared to cells from healthy controls and NOMID patients; more heterogeneity in osteoclast formation was observed in the DIRA patients (Figure 4A). Osteoclast function, assayed by bone resorption using a pit assay, showed higher bone resorption in the patient with Majeed syndrome and DIRA patients compared to the healthy controls and NOMID patients (Figure 4B).

RANK expression that accelerates osteogenesis (24) was increased in M2-MDMs from the patient with Majeed syndrome compared to healthy controls (Figure 4C), while overall IL-1R1 expression was comparable to that in healthy controls, with higher cell surface expression of IL-1R1 in the M2-MDMs from the patient with Majeed syndrome (Figure 4D). RANKL stimulation in healthy controls increased IL-1R1 surface expression (Supplementary Figure 7, <http://onlinelibrary.wiley.com/doi/10.1002/art.41624/abstract>), suggesting a role of RANKL in regulating surface expression of IL-1R1. Induction of IL-1R1 expression by c-Fos enabled IL-1-induced osteoclastogenesis in murine BMMs

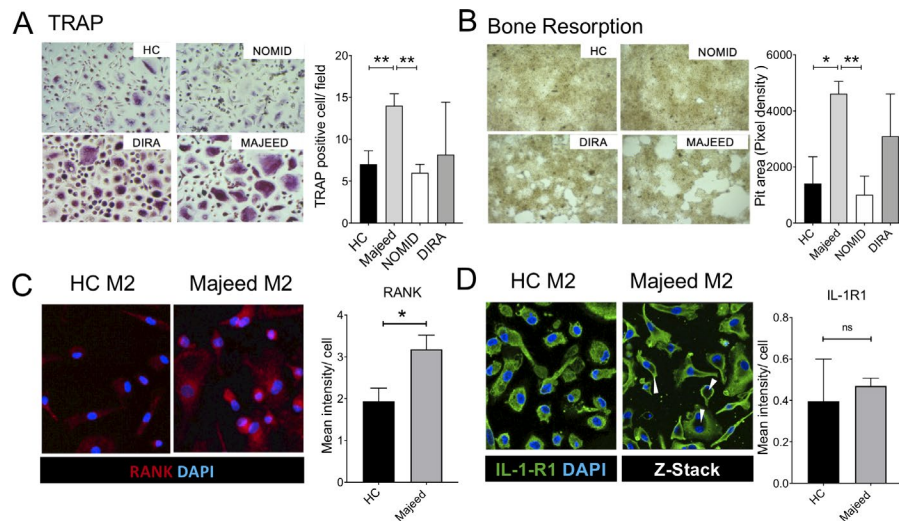


Figure 4. M2-like macrophages (M2-MDMs) in Majeed syndrome are more osteoclastogenic, and anakinra could reduce osteoclast fusion. **A**, MDMs were differentiated with macrophage colony-stimulating factor (M-CSF; 100 ng/ml) for 6 days and with a combination of M-CSF (100 ng/ml) and RANKL (30 ng/ml) for another 6 days, to differentiate them into osteoclasts. Tartrate-resistant alkaline phosphatase (TRAP)-positive multinucleated cells were quantified in the patient with Majeed syndrome, as well as in DIRA patients, healthy controls, and NOMID patients. **B**, Pit formation by osteoclasts was measured in macrophage cultures with fluoresceinamine-labeled chondroitin sulfate/calcium phosphate. In **A** and **B**, results are based on 3 independent experiments, with values shown as the mean \pm SD (healthy controls, $n = 4$; patient with Majeed syndrome, $n = 1$ with 2 visits; patients with NOMID, $n = 3$; and patients with DIRA, $n = 3$). **C** and **D**, M2-MDMs were stained for RANK expression on day 7 of culture with M-CSF (**C**) or stained for IL-1 receptor (IL-1R) (**D**). Nuclei were stained with DAPI. In **C** and **D**, results are based on 3 independent experiments, with values shown as the mean \pm SD intensity, quantified using Imaris software (version 9.2.1) (healthy controls, $n = 3$; patient with Majeed syndrome, $n = 1$). **Arrowheads** show the altered surface distribution of IL-1R in the patient's M2-MDMs compared to controls. In **A–D**, original magnification $\times 20$. * = $P < 0.05$; ** = $P < 0.001$, by Student's unpaired t -test. NS = not significant (see Figure 2 for other definitions).

in a RANKL/RANK-independent manner (24,25). In human cells, osteoclast differentiation was not induced by recombinant IL-1 β , independent of RANKL, nor did IL-1 β enhance RANKL-induced osteoclastogenesis (Supplementary Figure 8, <http://onlinelibrary.wiley.com/doi/10.1002/art.41624/abstract>). Binding of RANKL to its receptor (RANK) activates and/or induces expression of key transcription factors such as NF- κ B, c-Fos, melanocyte-inducing transcription factor, PU.1, and NFATc1, which is considered a master regulator of osteoclast differentiation in vitro and in vivo (26). NFATc1 orchestrates a signaling cascade that stimulates activator protein 1 and costimulatory signal-mediated intracellular Ca²⁺ oscillation (24,26,27). Consistent with these observations, NFATc1 was significantly up-regulated in the supernatant of LPS- and ATP-stimulated M2-MDMs and in osteoclasts from the patient with Majeed syndrome compared to healthy controls (Supplementary Figure 9, <http://onlinelibrary.wiley.com/doi/10.1002/art.41624/abstract>).

IL-1 inhibition effectively blocks proinflammatory cytokine production in M2-MDMs and accelerated osteoclastogenesis in the patient with Majeed syndrome. The clinical benefit of IL-1 blocking treatments in Majeed syndrome prompted investigation into the effect of IL-1 inhibition on stimulated cytokine and chemokine production in M2-MDMs and on osteoclastogenesis. IL-1 inhibition with anakinra significantly

reduced the production of inflammatory cytokines and osteoclastogenic chemokines in LPS- and ATP-stimulated M2-MDMs from the patient with Majeed syndrome and healthy controls, including the neutrophil-recruiting chemokines CXCL1/GRO α and IL-8, as well as IL-6, interferon- γ -inducible protein 10, TNF, and CCL5/RANTES (Figure 5A). In contrast, IL-10 levels remained low (data not shown). IL-1 inhibition with anakinra effectively reduced the number of TRAP-positive osteoclasts in a dose-dependent manner (Figure 5B), and the inhibitory effect was more pronounced in the patient with Majeed syndrome compared to healthy controls.

Although IL-1 β production increased during osteoclastogenesis, levels did not significantly differ between healthy controls and the patient with Majeed syndrome (Supplementary Figure 10A, <http://onlinelibrary.wiley.com/doi/10.1002/art.41624/abstract>). In contrast, the osteoclast differentiation factor MIF and serpin/plasminogen activator inhibitor (PAI) were induced in Majeed syndrome osteoclasts compared to healthy control osteoclasts (Supplementary Figures 10B and C). Similarly, osteoclastogenic factors CXCL1, CCL2/monocyte chemoattractant protein 1 (MCP-1), and CXCL8, which may function as autocrine factors in amplifying osteoclastogenesis, increased during osteoclast differentiation in the patient and controls (with higher levels in the patient with Majeed syndrome on day 8) (Supplementary Figures 10D–F). Osteoclastogenesis was inhibited by ISO-1 and anakinra, but it was less inhibited by tocilizumab, SPD304, and SP600125

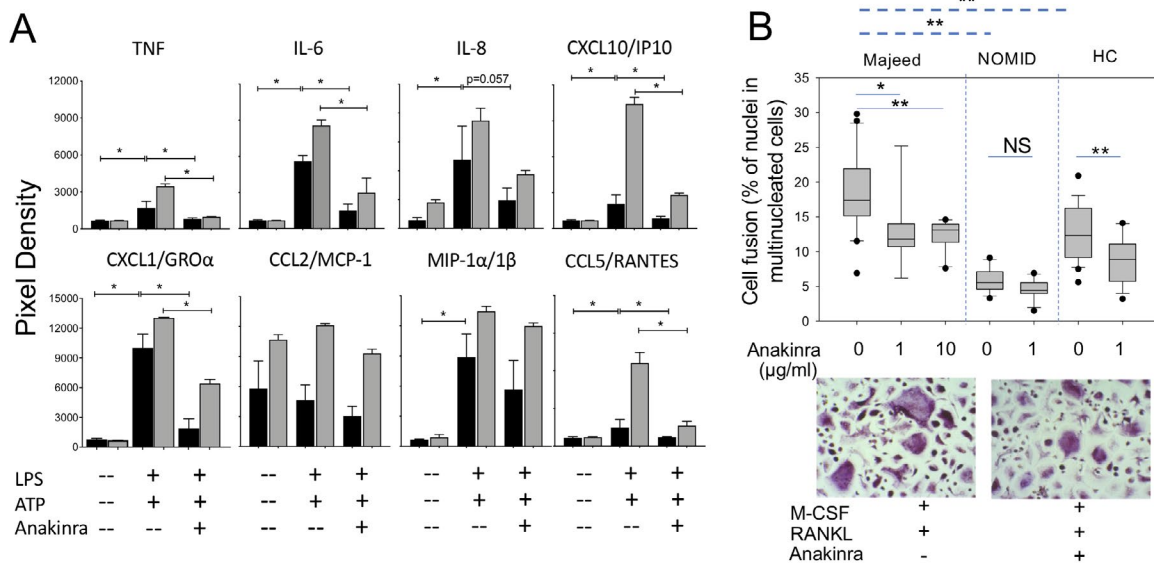


Figure 5. Effect of IL-1 blockade on osteoclastogenesis and proinflammatory cytokine/chemokine production by M2-MDMs. **A**, Monocyte-derived M2-MDMs were stimulated with LPS (1 μ g/ml) and ATP (1 mmole) for 24 hours, and LPS- and ATP-stimulated monocytes were cultured in the presence or absence of anakinra (10 μ g/ml). The relative levels of various cytokines and chemokines in supernatant were analyzed by antibody array, and intensities of cytokine expression were analyzed using ImageJ software. Bars show the mean \pm SD in cells from healthy controls ($n = 2$) (solid bars) and the patient with Majeed syndrome ($n = 1$ with 2 duplicates) (shaded bars). **B**, Monocytes from the patient with Majeed syndrome, patients with NOMID, and healthy controls were cultured with macrophage colony-stimulating factor (M-CSF) for 6 days, then RANKL was added to the M-CSF, and, simultaneously, M2-MDMs were cultured in the presence or absence of anakinra (1 mg/ml or 10 mg/ml). After 6 days, small and large tartrate-resistant alkaline phosphatase-positive cells with >3 nuclei were quantified. Data are shown as box plots, where the boxes represent the 25th to 75th percentiles, the lines within the boxes represent the median, and the lines outside the boxes represent the minimum and maximum values (healthy controls [$n = 3$], NOMID patients [$n = 3$], patient with Majeed syndrome [$n = 1$ with 2 duplicates]). Original magnification $\times 20$. * = $P < 0.05$; ** = $P < 0.001$. TNF = tumor necrosis factor; IP-10 = interferon- γ -inducible protein 10; GRO α = growth-related oncogene α ; MCP-1 = monocyte chemoattractant protein 1; NS = not significant (see Figure 2 for other definitions).

(Figure 6A). Anakinra reduced MIF, serpin/PAI, and intercellular adhesion molecule 1 production during osteoclastogenesis more effectively than IL-6 inhibition (Supplementary Figure 11, <http://onlinelibrary.wiley.com/doi/10.1002/art.41624/abstract>), and may block osteoclastogenesis by reducing autocrine production of the osteoclastogenic factors MIF and serpin/PAI.

LPIN2 mutations affect M2-MDM activation and osteoclast differentiation by modification of phosphokinase activity of JNK/MAPKs and Src kinases.

Lipin 2 depletion leads to accumulation of phosphatidic acid, which activates the JNK 1/c-Jun pathway to induce transcription of proinflammatory cytokine genes including IL-6, CCL-2/MCP-1, and TNF in macrophage cell lines (28). Activation of several JNK/MAPKs is known to promote osteoclast differentiation (28–34). We hypothesized that the chemokine dysregulation and/or osteoclast differentiation may be mediated by up-regulation of JNK/MAPK pathways and screened for differences in site-specific phosphorylation in 43 kinases in M2-MDMs. Of those screened, 9 were differentially phosphorylated (Figure 6B). Site-specific phosphorylation was increased in JNK1/2/3, MSK1/2, FAK, PRAS40, mechanistic target of rapamycin (mTOR), and STAT5b in the M2-MDMs from the patient with Majeed syndrome compared to healthy controls.

Phosphorylation was unchanged in the Src family kinase member Hck and the multifunctional Ser/Thr protein kinase glycogen synthase kinase 3 α/β . In contrast, c-Src kinase phosphorylation at position p.Y419, which is essential for full activation (35), was markedly reduced in the patient with Majeed syndrome compared to healthy controls. Phosphorylation was also lower in Pyk-2 and WNK1 in the patient compared to healthy controls (Figure 6B). Overall, our data suggest that disease-causing *LPIN2* mutations alter bone homeostasis by modulating phosphokinase activity in M2-MDMs, thus accelerating osteoclastogenesis. The proinflammatory effect of the *LPIN2* mutation on M2-MDMs and osteoclasts was inhibited by IL-1 blockade with anakinra.

DISCUSSION

Majeed syndrome is caused by loss-of-function mutations in *LPIN2*, and disease-causing mutations are recessive and include missense mutations at positions p.S734L or p.R736H or truncating mutations at positions p.C181*, p.S439Wfs*, p.R564Kfs*3, p.Y747*, and p.R776Sfs*66 (Supplementary Table 2, <http://onlinelibrary.wiley.com/doi/10.1002/art.41624/abstract>). This is the first report of an American patient with Majeed syndrome who is compound heterozygous, exhibiting a previously undescribed 17.8-kb deletion of exons

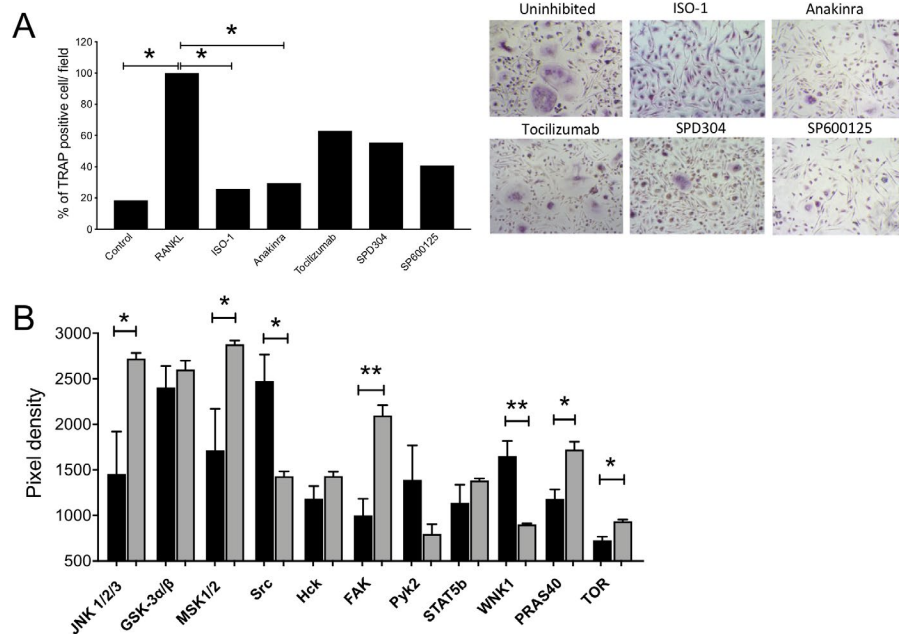


Figure 6. IL-1 and macrophage migration inhibitory factor (MIF) blockade inhibit osteoclastogenesis, and mutant lipin 2 regulates proinflammatory M2-like macrophages (M2-MDMs) by altering JNK/MAPK expression. **A**, IL-1 inhibition with anakinra and MIF inhibition with ISO-1 inhibited osteoclastogenesis most effectively. Macrophages were differentiated into osteoclasts. Cells were left untreated or treated with a MIF inhibitor (ISO-1; 100 μ M), an IL-1 inhibitor (anakinra; 1 mg/ml), an IL-6 inhibitor (tocilizumab; 10 mg/ml), a tumor necrosis factor inhibitor (SPD304; 5 μ M), or a JNK inhibitor (SP600125; 10 μ M). All experiments were performed in cells from healthy controls. Tartrate-resistant alkaline phosphatase (TRAP)-positive multinucleated cells with >3 nuclei were quantified. Bars show the mean of triplicate assays. Original magnification $\times 100$. **B**, The Human Phospho-Kinase Array was used to detect multiple phosphorylated kinases in macrophages in the sample from the patient with Majeed syndrome (shaded bars) and healthy controls (solid bars), differentiated with macrophage colony-stimulating factor (100 ng/ml) for 6 days. Cell lysate (60 μ l) was analyzed to detect the phosphorylation state of M2-MDMs at the basal level. Spot densities of phosphoproteins were quantified using ImageJ software. Bars show the mean \pm SD of 2 independent experiments, with duplicates for the patient with Majeed syndrome. * = $P < 0.05$; ** = $P < 0.001$, by Student's unpaired t -test. GSK-3 α/β = glycogen synthase kinase 3 α/β ; TOR = mechanistic target of rapamycin (see Figure 2 for other definitions).

7–18 and a novel missense mutation at position 517 that affects a splice site that alternatively splices out exon 10, or exons 10 and 11. The 17.8-kb deletion may be missed with targeted and whole-exome sequencing techniques. Treatment with IL-1 blocking agents reverts the inflammatory bone disease and normalizes the acute-phase reactants, emphasizing the need for a rapid diagnosis.

While IL-1-mediated autoinflammatory diseases including NOMID and DIRA share significant systemic inflammation with granulocytosis and elevated acute-phase reactant levels, only patients with DIRA or Majeed syndrome (but not cryopyrinopathies such as NOMID) develop osteomyelitis (Supplementary Figure 1, <http://online.library.wiley.com/doi/10.1002/art.41624/abstract>). The inflammatory bone lesions in patients with Majeed syndrome primarily localize to the growth plates of long bones, which prompted the evaluation of the role of disease-causing *LPIN2* mutations in molecular mechanisms that regulate bone homeostasis, specifically the polarization of regulatory M2-MDMs. Consistent with other IL-1-mediated autoinflammatory diseases, Majeed syndrome M1-MDMs secreted more IL-1 β compared to M1-MDMs from healthy controls but less than NOMID M1-MDMs.

In contrast, antiinflammatory or regulatory M2-MDMs from the patient with Majeed syndrome secreted high levels of

proinflammatory cytokine IL-6 and chemokines IL-8, CCL2/MCP-1, CXCL1/GRO α , CCL5/RANTES, and CXCL10. Many were also increased in DIRA patients, but not in NOMID and healthy control M2-MDMs, suggesting that the inflammatory M2-MDM phenotype cannot be attributed to inflammasome activation. In fact, IL-8 (36), CCL2/MCP-1 (37,38), MIP-1 α/β (39), and CCL5/RANTES (21), which were elevated in LPS- and ATP-stimulated Majeed syndrome M2-MDMs, accelerate osteoclast differentiation and have been associated with the progression of metastatic bone lesions. These osteoclastogenic factors may act in a paracrine manner, promoting osteoclastogenesis at the growth plate. CCL2/MCP-1 recruits monocytes that differentiate into tissue macrophages, and IL-8 and CXCL1, both prominent neutrophil-attracting chemokines, may orchestrate the recruitment of neutrophils into the growth plate, which is the hallmark of sterile osteomyelitis and is absent in conditions of exclusive osteoclast activation (such as osteoporosis).

Osteoclastogenesis was enhanced in the patient with Majeed syndrome, independently of the aforementioned cytokines and chemokines. The enhanced osteoclastogenesis in this patient and those with DIRA was significantly reduced by IL-1 blockade with anakinra. Mechanisms by which IL-1 blockade controls bone inflammation remain incompletely understood. However, the

increase in RANKL and in the induction of NFATc1, a master regulator of osteoclastogenesis, as well as the increased surface distribution of IL-1R1, suggest a role of intracellular signaling pathways that accelerate osteoclastogenesis independently of autocrine production of osteoclastic factors. These factors also illustrate a complex role of lipin 2 deficiency in regulating bone inflammation that includes the induction of RANK in M2-MDMs. This was consistent with the relatively small effect of culture supernatant from the patient with Majeed syndrome on enhancing osteoclastogenesis in vitro (data not shown).

Lipin 2 has emerged as a metabolic checkpoint that links fatty acid metabolism to proinflammatory signaling in macrophages (28), by controlling the cellular concentrations of DAG and phosphatidic acid in saturated fatty acid–overloaded macrophages (40–42). In models of *Lpin2* deficiency, the reduced phosphatidic acid phosphatase activity results in decreased DAG production and phosphatidic acid accumulation, which can activate ERK/JNK signaling pathways (13). Consistent with these findings, JNK and MSK1/2 phosphorylation, which promote proinflammatory chemokine/cytokine production in adaptive and innate immune cells (43,44), was increased in the M2-MDMs from the patient with Majeed syndrome. In contrast, the profound decrease in Src kinase phosphorylation at p.Y419 in the patient's M2-MDMs had not previously been implicated with lipin 2 deficiency. Src activation is essential for regulating the antiinflammatory property of M2-MDMs and for promoting M2-MDM polarization by increasing IL-10 production (45) and by promoting the production of IL-4–induced STAT6 and Jak1-dependent arginase 1 (46). The low IL-10 secretion and CD163 expression in Majeed syndrome M2-MDMs, which were not corrected by IL-1 inhibition (data not shown), are likely caused by the profound suppression of Src phosphorylation (47) and are consistent with low levels of Pyk-2 phosphorylation (48,49) also observed in the patient with Majeed syndrome.

Src is also a central regulator of osteoclast resorption (50–53), but we did not assess Src phosphorylation in mature osteoclasts. In contrast, FAK, PRAS40, mTOR, and STAT5b kinases (which play a role in cell spreading, migration, and survival in tumor cells [47,54–59], in regulating mTORC1-dependent polarization of macrophages [60,61], and in osteoclastogenesis [62]) were increased in the M2-MDMs from the patient with Majeed syndrome. Although we did not assess the effect of IL-1 blockade on modulating kinase phosphorylation, the significant suppression of proinflammatory cytokine production and bone differentiation factors MIF and serpin/PAI with IL-1 blockade is likely regulated through modulation of phosphokinases (63). Our findings add to recently published data on a novel genetic cause of multifocal osteomyelitis that illustrate the relevance of another Src kinase, Fgr, in promoting osteoclastogenesis (64).

Bone-resident tissue macrophages recently referred to as “osteomacs” (65) have been proposed to have a pivotal role in regulating bone homeostasis. Osteomacs form canopy-like structures

at bone remodeling sites, are CD68-positive, and TRAP-negative (66,67). Their distinctive stellate and spindle-shaped morphology makes it intriguing to speculate that *LPIN2* mutations influencing the polarization of the spindle-like M2-MDMs in our in vitro culture system may regulate the inflammatory polarization of osteomacs in vivo, thus regulating bone inflammation in patients with Majeed syndrome. Since bone biopsies were not available and *Lpin2*^{-/-} murine models do not develop osteomyelitis, this hypothesis has not been further investigated.

Limitations of our study include the evaluation of only 1 patient with Majeed syndrome; however, the inclusion of monogenic controls, particularly NOMID and DIRA patients, and normal controls demonstrates disease-specific clustering. The absence of osteomyelitis in *Lpin2*^{-/-} mice further limits the ability to evaluate the bone phenotype.

Taken together, our data suggest that lipin 2 modulates bone homeostasis independently of inflammasome activation by driving osteoclastogenesis and altering phosphorylation of JNK and Src kinases that render regulatory M2-MDMs inflammatory and accelerate osteoclastogenesis. We propose a model for sterile osteomyelitis that illustrates the important role of phosphokinases in modulating the inflammatory properties of M2-MDMs and osteoclastogenesis (Supplementary Figure 12, <http://onlinelibrary.wiley.com/doi/10.1002/art.41624/abstract>). Our data may assist in characterizing pathways and identifying genetic causes for clinically or genetically uncharacterized conditions presenting with chronic recurrent multifocal osteomyelitis and suggest additional targets for treatment.

ACKNOWLEDGMENTS

The authors would like to thank Drs. Sally Hunsberger and Paul Wakim for review of the statistical analyses.

AUTHOR CONTRIBUTIONS

All authors were involved in drafting the article or revising it critically for important intellectual content, and all authors approved the final version to be published. Dr. Goldbach-Mansky had full access to all of the data in the study and takes responsibility for the integrity of the data and the accuracy of the data analysis.

Study conception and design. Bhuyan, de Jesus, Ferguson, Goldbach-Mansky.

Acquisition of data. Bhuyan, de Jesus, Mitchell, Leikina, VanTries, Herzog, Onel, Oler, Montealegre Sanchez, Johnson, Bichell, Marrero, Fernandez De Castro, Huang, Ganesan.

Analysis and interpretation of data. Bhuyan, de Jesus, Calvo, Collins, Ganesan, Chernomordik, Ferguson, Goldbach-Mansky.

REFERENCES

- De Jesus AA, Canna SW, Liu Y, Goldbach-Mansky R. Molecular mechanisms in genetically defined autoinflammatory diseases: disorders of amplified danger signaling [review]. *Annu Rev Immunol* 2015;33:823–74.
- Ferguson PJ, Chen S, Tayeh MK, Ochoa L, Leal SM, Pelet A, et al. Homozygous mutations in *LPIN2* are responsible for the syndrome of chronic recurrent multifocal osteomyelitis and congenital dyserythropoietic anaemia (Majeed syndrome). *J Med Genet* 2005; 42:551–7.

3. Aksentijevich I, Masters SL, Ferguson PJ, Dancy P, Frenkel J, van Royen-Kerkhoff A, et al. An autoinflammatory disease with deficiency of the interleukin-1-receptor antagonist. *N Engl J Med* 2009;360:2426–37.
4. Reddy S, Jia S, Geoffrey R, Lorier R, Suchi M, Broeckel U, et al. An autoinflammatory disease due to homozygous deletion of the *IL1RN* locus. *N Engl J Med* 2009;360:2438–44.
5. Majeed HA, Kalaawi M, Mohanty D, Teebi AS, Tunjekar MF, al-Gharbawy F, et al. Congenital dyserythropoietic anemia and chronic recurrent multifocal osteomyelitis in three related children and the association with Sweet syndrome in two siblings. *J Pediatr* 1989;115:730–4.
6. Herlin T, Fiirgaard B, Bjerre M, Kerndrup G, Hasle H, Bing X, et al. Efficacy of anti-IL-1 treatment in Majeed syndrome. *Ann Rheum Dis* 2013;72:410–3.
7. Liu J, Hu XY, Zhao ZP, Guo RL, Guo J, Li W, et al. Compound heterozygous *LPIN2* pathogenic variants in a patient with Majeed syndrome with recurrent fever and severe neutropenia: case report. *BMC Med Genet* 2019;20:182.
8. Peterfy M, Phan J, Xu P, Reue K. Lipodystrophy in the fld mouse results from mutation of a new gene encoding a nuclear protein, lipin [letter]. *Nat Genet* 2001;27:121–4.
9. Stein Y, Shapiro B. The synthesis of neutral glycerides by fractions of rat liver homogenates. *Biochim Biophys Acta* 1957;24:197–8.
10. Han GS, Wu WI, Carman GM. The *Saccharomyces cerevisiae* Lipin homolog is a Mg²⁺-dependent phosphatidate phosphatase enzyme. *J Biol Chem* 2006;281:9210–8.
11. Kok BP, Venkatraman G, Capatos D, Brindley DN. Unlike two peas in a pod: lipid phosphate phosphatases and phosphatidate phosphatases [review]. *Chem Rev* 2012;112:5121–46.
12. Reue K, Brindley DN. Thematic review series: glycerolipids. Multiple roles for lipins/phosphatidate phosphatase enzymes in lipid metabolism. *J Lipid Res* 2008;49:2493–503.
13. Lorden G, Sanjuan-Garcia I, de Pablo N, Meana C, Alvarez-Miguel I, Perez-Garcia MT, et al. Lipin-2 regulates NLRP3 inflammasome by affecting P2X7 receptor activation. *J Exp Med* 2017;214:511–28.
14. Hashimoto M, Nasser H, Chihara T, Suzu S. Macropinocytosis and TAK1 mediate anti-inflammatory to pro-inflammatory macrophage differentiation by HIV-1 Nef. *Cell Death Dis* 2014;5:e1267.
15. Verma SK, Chernomordik LV, Melikov K. An improved metrics for osteoclast multinucleation. *Sci Rep* 2018;8:1768.
16. Hashimoto M, Nasser H, Bhuyan F, Kuse N, Satou Y, Harada S, et al. Fibrocytes differ from macrophages but can be infected with HIV-1. *J Immunol* 2015;195:4341–50.
17. Eckert MA, Coscia F, Chryplewicz A, Chang JW, Hernandez KM, Pan S, et al. Proteomics reveals NNMT as a master metabolic regulator of cancer-associated fibroblasts. *Nature* 2019;569:723–8.
18. Amarasekara DS, Yun H, Kim S, Lee N, Kim H, Rho J. Regulation of osteoclast differentiation by cytokine networks [review]. *Immune Netw* 2018;18:e8.
19. Kwak HB, Ha H, Kim HN, Lee JH, Kim HS, Lee S, et al. Reciprocal cross-talk between RANKL and interferon- γ -inducible protein 10 is responsible for bone-erosive experimental arthritis. *Arthritis Rheum* 2008;58:1332–42.
20. Lee JH, Kim HN, Kim KO, Jin WJ, Lee S, Kim HH, et al. CXCL10 promotes osteolytic bone metastasis by enhancing cancer outgrowth and osteoclastogenesis. *Cancer Res* 2012;72:3175–86.
21. Sucer A, Jajic Z, Artukovic M, Matijasevic MI, Anic B, Flegar D, et al. Chemokine signals are crucial for enhanced homing and differentiation of circulating osteoclast progenitor cells. *Arthritis Res Ther* 2017;19:142.
22. Wiktor-Jedrzejczak W, Bartocci A, Ferrante AW Jr, Ahmed-Ansari A, Sell KW, Pollard JW, et al. Total absence of colony-stimulating factor 1 in the macrophage-deficient osteopetrotic (op/op) mouse. *Proc Natl Acad Sci U S A* 1990;87:4828–32.
23. Boyle WJ, Simonet WS, Lacey DL. Osteoclast differentiation and activation. *Nature* 2003;423:337–42.
24. Park JH, Lee NK, Lee SY. Current understanding of RANK signaling in osteoclast differentiation and maturation. *Mol Cells* 2017;40:706–13.
25. Kim JH, Jin HM, Kim K, Song I, Youn BU, Matsuo K, et al. The mechanism of osteoclast differentiation induced by IL-1. *J Immunol* 2009;183:1862–70.
26. Takayanagi H, Kim S, Koga T, Nishina H, Isshiki M, Yoshida H, et al. Induction and activation of the transcription factor NFATc1 (NFAT2) integrate RANKL signaling in terminal differentiation of osteoclasts. *Dev Cell* 2002;3:889–901.
27. Kim JH, Kim N. Regulation of NFATc1 in osteoclast differentiation. *J Bone Metab* 2014;21:233–41.
28. Valdearcos M, Esquinas E, Meana C, Pena L, Gil-de-Gomez L, Balsinde J, et al. Lipin-2 reduces proinflammatory signaling induced by saturated fatty acids in macrophages. *J Biol Chem* 2012;287:10894–904.
29. David JP, Sabapathy K, Hoffmann O, Idarraga MH, Wagner EF. JNK1 modulates osteoclastogenesis through both c-Jun phosphorylation-dependent and -independent mechanisms. *J Cell Sci* 2002;115:4317–25.
30. Ikeda F, Matsubara T, Tsurukai T, Hata K, Nishimura R, Yoneda T. JNK/c-Jun signaling mediates an anti-apoptotic effect of RANKL in osteoclasts. *J Bone Miner Res* 2008;23:907–14.
31. Yamanaka Y, Abu-Amer Y, Faccio R, Clohisey JC. Map kinase c-JUN N-terminal kinase mediates PMMA induction of osteoclasts. *J Orthop Res* 2006;24:1349–57.
32. Li X, Udagawa N, Itoh K, Suda K, Murase Y, Nishihara T, et al. p38 MAPK-mediated signals are required for inducing osteoclast differentiation but not for osteoclast function. *Endocrinology* 2002;143:3105–13.
33. Kobayashi N, Kadono Y, Naito A, Matsumoto K, Yamamoto T, Tanaka S, et al. Segregation of TRAF6-mediated signaling pathways clarifies its role in osteoclastogenesis. *EMBO J* 2001;20:1271–80.
34. Teitelbaum SL, Ross FP. Genetic regulation of osteoclast development and function [review]. *Nat Rev Genet* 2003;4:638–49.
35. Zhang Y, Tu Y, Zhao J, Chen K, Wu C. Reversion-induced LIM interaction with Src reveals a novel Src inactivation cycle. *J Cell Biol* 2009;184:785–92.
36. Bendre MS, Margulies AG, Walsler B, Akel NS, Bhattacharya S, Skinner RA, et al. Tumor-derived interleukin-8 stimulates osteolysis independent of the receptor activator of nuclear factor- κ B ligand pathway. *Cancer Res* 2005;65:11001–9.
37. Li X, Loberg R, Liao J, Ying C, Snyder LA, Pienta KJ, et al. A destructive cascade mediated by CCL2 facilitates prostate cancer growth in bone. *Cancer Res* 2009;69:1685–92.
38. Zhang J, Patel L, Pienta KJ. CC chemokine ligand 2 (CCL2) promotes prostate cancer tumorigenesis and metastasis [review]. *Cytokine Growth Factor Rev* 2010;21:41–8.
39. Roodman GD. Biology of osteoclast activation in cancer. *J Clin Oncol* 2001;19:3562–71.
40. Balboa MA, Balsinde J, Dennis EA. Involvement of phosphatidate phosphohydrolase in arachidonic acid mobilization in human amniotic WISH cells. *J Biol Chem* 1998;273:7684–90.
41. Balboa MA, Balsinde J, Dennis EA, Insel PA. A phospholipase D-mediated pathway for generating diacylglycerol in nuclei from Madin-Darby canine kidney cells. *J Biol Chem* 1995;270:11738–40.
42. Balsinde J, Balboa MA, Insel PA, Dennis EA. Differential regulation of phospholipase D and phospholipase A2 by protein kinase C in P388D1 macrophages. *Biochem J* 1997;321:805–9.
43. Arthur JS. MSK activation and physiological roles. *Front Biosci* 2008;13:5866–79.
44. Kitanaka T, Nakano R, Kitanaka N, Kimura T, Okabayashi K, Narita T, et al. JNK activation is essential for activation of MEK/ERK signaling

- in IL-1 β -induced COX-2 expression in synovial fibroblasts. *Sci Rep* 2017;7:39914.
45. Hu X, Han C, Jin J, Qin K, Zhang H, Li T, et al. Integrin CD11b attenuates colitis by strengthening Src-Akt pathway to polarize anti-inflammatory IL-10 expression. *Sci Rep* 2016;6:26252.
 46. Hu X, Wang H, Han C, Cao X. Src promotes anti-inflammatory (M2) macrophage generation via the IL-4/STAT6 pathway. *Cytokine* 2018;111:209–15.
 47. Buechler C, Ritter M, Orso E, Langmann T, Klucken J, Schmitz G. Regulation of scavenger receptor CD163 expression in human monocytes and macrophages by pro- and antiinflammatory stimuli. *J Leukoc Biol* 2000;67:97–103.
 48. Sanjay A, Houghton A, Neff L, DiDomenico E, Bardelay C, Antoine E, et al. Cbl associates with Pyk2 and Src to regulate Src kinase activity, $\alpha(v)\beta(3)$ integrin-mediated signaling, cell adhesion, and osteoclast motility. *J Cell Biol* 2001;152:181–95.
 49. Zhao M, Finlay D, Zharkikh I, Vuori K. Novel role of Src in priming Pyk2 phosphorylation. *PLoS One* 2016;11:e0149231.
 50. Thomas SM, Brugge JS. Cellular functions regulated by Src family kinases. *Annu Rev Cell Dev Biol* 1997;13:513–609.
 51. Boyce BF, Yoneda T, Lowe C, Soriano P, Mundy GR. Requirement of pp60c-src expression for osteoclasts to form ruffled borders and resorb bone in mice. *J Clin Invest* 1992;90:1622–7.
 52. Lowe C, Yoneda T, Boyce BF, Chen H, Mundy GR, Soriano P. Osteopetrosis in Src-deficient mice is due to an autonomous defect of osteoclasts. *Proc Natl Acad Sci U S A* 1993;90:4485–9.
 53. Aleshin A, Finn RS. SRC: a century of science brought to the clinic [review]. *Neoplasia* 2010;12:599–607.
 54. Carron JD, Greinwald JH, Oberman JP, Werner AL, Derkay CS. Simulated reflux and laryngotracheal reconstruction: a rabbit model. *Arch Otolaryngol Head Neck Surg* 2001;127:576–80.
 55. Fregosi RF, Hwang JC, Bartlett D Jr, St. John WM. Activity of abdominal muscle motoneurons during hypercapnia. *Respir Physiol* 1992;89:179–94.
 56. Xiong WC, Feng X. PYK2 and FAK in osteoclasts. *Front Biosci* 2003;8:d1219–26.
 57. Miyazaki T, Sanjay A, Neff L, Tanaka S, Horne WC, Baron R. Src kinase activity is essential for osteoclast function. *J Biol Chem* 2004;279:17660–6.
 58. Miyazaki T, Tanaka S, Sanjay A, Baron R. The role of c-Src kinase in the regulation of osteoclast function. *Mod Rheumatol* 2006;16:68–74.
 59. Ray BJ, Thomas K, Huang CS, Gutknecht MF, Botchwey EA, Bouton AH. Regulation of osteoclast structure and function by FAK family kinases. *J Leukoc Biol* 2012;92:1021–8.
 60. Nascimento EB, Snel M, Guigas B, van der Zon GC, Kriek J, Maassen JA, et al. Phosphorylation of PRAS40 on Thr246 by PKB/AKT facilitates efficient phosphorylation of Ser183 by mTORC1. *Cell Signal* 2010;22:961–7.
 61. Byles V, Covarrubias AJ, Ben-Sahra I, Lamming DW, Sabatini DM, Manning BD, et al. The TSC-mTOR pathway regulates macrophage polarization. *Nat Commun* 2013;4:2834.
 62. Kim JH, Sim JH, Lee S, Seol MA, Ye SK, Shin HM, et al. Interleukin-7 induces osteoclast formation via STAT5, independent of receptor activator of NF- κ B ligand. *Front Immunol* 2017;8:1376.
 63. Granata F, Frattini A, Loffredo S, del Prete A, Sozzani S, Marone G, et al. Signaling events involved in cytokine and chemokine production induced by secretory phospholipase A2 in human lung macrophages. *Eur J Immunol* 2006;36:1938–50.
 64. Abe K, Cox A, Takamatsu N, Velez G, Laxer RM, Tse SM, et al. Gain-of-function mutations in a member of the Src family kinases cause autoinflammatory bone disease in mice and humans. *Proc Natl Acad Sci U S A* 2019;116:11872–7.
 65. Gu Q, Yang H, Shi Q. Macrophages and bone inflammation. *J Orthop Translat* 2017;10:86–93.
 66. Sinder BP, Pettit AR, McCauley LK. Macrophages: their emerging roles in bone [review]. *J Bone Miner Res* 2015;30:2140–9.
 67. Chang MK, Raggatt LJ, Alexander KA, Kuliwaba JS, Fazzalari NL, Schroder K, et al. Osteal tissue macrophages are intercalated throughout human and mouse bone lining tissues and regulate osteoblast function in vitro and in vivo. *J Immunol* 2008;181:1232–44.